eduFRET: a FRET Microscope for Educational Use

Kaitlyn Alexa Gabardi[1]*, Kadina Elizabeth Johnston[1]*, Ethan Thomas Nethery[1]*, Benjamin A. Ratliff[1]*, John Walker Rupel II[1]*, Jeremy D. Rogers[1], and Matthew J. Merrins[2]

[1]Department of Biomedical Engineering, University of Wisconsin-Madison, Madison, WI 53715, USA
[2]Department of Medicine, University of Wisconsin-Madison, Madison, WI, 53715, USA
*Indicates equal contribution

Abstract

The eduFRET is an affordable, fluorescence resonance energy transfer microscope that offers a cheaper alternative for students to gain hands-on experience working with research relevant to this topic. This scope implements a unique imaging algorithm that is combined with optics and mechanics structured to accurately measure fluorescence resonance energy transfer in different experiments. The software and optical resolutions were both tested, and it was concluded that the eduFRET is capable of accurately measuring the energy transfer and quantitative reporting. This microscope is intended to be implemented as a cost-effective teaching tool to introduce the techniques of microscopy to students who are interested in biomedical and drug discovery research.

Introduction

Biosensors are powerful tools for monitoring intracellular processes, and they have been growing in popularity as protein engineering techniques improve, being implemented in a variety of industries [1, 2]. Genetically encoded biosensors are a subcategory that includes a variety of fluorescent proteins including the ubiquitous green fluorescent protein, GFP [3]. Because of their versatility for use in quantitative plate reader assays or for microscopy imaging, fluorescent biosensors have been applied to a variety of intracellular monitoring systems including transcriptional regulation and protein dynamics [4-11]. To monitor spatial dynamics or protein-protein interactions, fluorophores can be linked to the proteins of interest [12]. Alternatively, to monitor intracellular concentrations or substrates, a binding site for the protein of interest can be fused within the sequence of the fluorophore, such that binding influences the intensity of emission and can be correlated to substrate concentration. Binding causes a

conformational change that either brings the two parts of the protein together to increase fluorescence, or separates them to decrease it. These types of sensors can be difficult to build since the insertion point for the binding site must be found through trial and error, and may not work at all due to the complex relationship between sequence, structure, and function [13]. Another type of biosensor utilizes two fluorescent proteins which are attached on either side of the binding domain directly or by linking peptide chains [14-21] . These sensors use the theory behind fluorescence resonance energy transfer (FRET) to give a quantitative method of determining intracellular concentrations [13].

FRET works on the basis of light transfer between two fluorophores [22]. The first fluorophore, referred to as the donor fluorophore, is excited at a specific wavelength of light by an LED or laser, usually near the ultraviolet range [13, 23]. When this light interacts with the donor fluorophore, it is excited, and when it de-excites it emits light at a lower wavelength than the original incident rays. The second fluorophore is the acceptor, which is excited at the same wavelength that the donor emits. If it is in close enough proximity to the donor, it absorbs the light by energy transfer. Upon de-excitation it will emit a lower wavelength of light [13]. During this process, the intensity of emission of both of the fluorophores can be monitored with the proper microscopy equipment, and from these intensities a FRET ratio can be calculated [23]. This ratio is indicative of the amount of energy transfer between the two fluorophores, and generally changes by about 10% [24]. On biosensors, binding and dissociation of a ligand causes the two fluorophores to move closer or further away from each other, directly or inversely impacting the efficiency of the energy transfer. The FRET ratio will decrease with increasing distance between the two fluorophores [25]. This results in a quantitative relationship between the calculated FRET ratio and the ligand concentration [23].

Microscopes capable of measuring FRET are used primarily for research and are designed to perform multiple types of microscopy. This makes them more expensive and not ideal for educational purposes. The microscope designed specifically is used to perform FRET with a specific biosensor, called laconic, which is composed of the two fluorophores, monomeric teal fluorescent protein (mTFP) and venus, a yellow fluorescent protein, linked by a lactate binding domain [23]. mTFP is the donor fluorophore, which is excited by light between 400 and 470 nm, and emits light between 460 nm and 550 nm [26]. Venus is our acceptor fluorophore, which is excited in the range of 475 nm to 530 nm and emits light between 500 and 535 nm. In Laconic, the fluorophores on the unbound sensor are in the optimal positions for FRET to occur; upon lactate binding there is a conformational change that separates the fluorophores and decreases transfer efficiency.

Therefore this design only requires one set of fluorescence filters compared to the multiple filter sets used in traditional FRET microscope. The eduFRET works by exciting a specimen with a 420 nm LED. The light from the LED passes through a collimator to ensure the specimen is evenly illuminated. The excitation light then travels through a 430 filter, reflects off a triple bandpass dichroic mirror, and travels through an objective lens. The specimen, infected with a laconic sensor, will emit 470 nm and 535 nm. These wavelengths will pass off the dichroic mirror and reflect off the fold mirror. The emitted light will then travel through either a 535 nm filter or a 470 nm filter. Finally the light pass through a tube lens which focuses the light to form an image on the camera. To calculate the FRET ratio two images are acquired one with the 535 nm filter in place and one with the 470 nm filter in place. The images are then ran through an algorithm that outputs a FRET ratio. A time lapse functionality built into the microscope will allow users of the microscope to measure changes FRET ratio over time.

Materials and methods

Optical Components

The tube lens used was a 100 mm achromatic lens (Edmund Optics, 47-641). The objective used was a 20x 0.75 NA Plan from Nikon. The field of view with a 100 mm tube lense and the 40x Plan Olympus is 0.480 mm X 0.360 mm. Two sets of filters were provided by Merrins Lab, University of Wisconsin-Madison, in order to design an epi-fluorescent microscope. For the purpose of this device, a 430 nm wavelength excitation filter is needed in order to excite the mTFP fluorophore appropriately. The two emission filters provided filtered light centered at 470 nm and 535 nm. The excitation and emission filters are held in the microscope in a Dual-Position Slider Bundle (Thorlabs, ELL6K), which is controllable with the eduFRET's packaged software. The sample is excited by one 420 nm 3W Vollong high powered LED. Details on the power source circuit can be found in Figure 1. A 35 mm achromatic doublet lens (Edmund Optics, 32-319) was used to collimate the light exiting the source. A fold mirror was purchased (Thorlabs, PFR10-P01) in order to condense the height of the microscope. A triple bandpass ECFP/EYFP/mCherry filter (Chroma, 69008) was purchased. Two dichroic filter cubes (Thorlabs, CM1-DCH) were also purchased to hold the cube. The camera used was the DMK42BUC03. The pixel size of the camera is 3.75 x 3.75 μm, and the sensor size is 4.8 x 3.6 mm. The quantum efficiency of the camera is above 64% and between 450 nm and 600 nm. The z-axis of the microscope was purchased (AmScope, FR-A1), and a 3D printed cell dish holder was printed at UW Madison's MakerSpace using PLA and PVA supports (See S1 in supplemental material). The final assembly of the microscope can be seen in S2 of supplementary material.

Image Processing Algorithm

To permit for easy control of the electro-mechanical devices and streamline calculation and analysis of the images collected, a Graphical User Interface (GUI) was developed. To analyze the images gathered, a basic FRET ratio calculation algorithm was developed within the GUI for single image pair analysis and timelapse-image pair analysis series.

Using EmguCV, a C# wrapper for the OpenCV image processing toolbox, images taken from the CFP and YFP channels were loaded as separate arrays. The image backgrounds are then subtracted from images. These images are then thresholded to reduce the noise in the images by removing background regions of the images that do not display any protein fluorescence. The remaining indexed values of interest are divided between CFP/YFP channels, and their averaged value is displayed to the user on the GUI. A .csv file containing a collection of the FRET ratios for each image pair taken during the time-lapsed experiment is automatically created.

A testing protocol was developed to determine the efficacy of the imaging algorithm with respect to commercial software. Using a Nikon TI Eclipse microscope, time-lapse images of pancreatic islet cells exposed to varied glucose concentration were collected over a duration of roughly 10 minutes. Three treatments were implemented with varying transitions between high glucose concentration, 16.2 mM, and low glucose concentration, 2 mM. The first and fourth treatment consisted of a gradual transition from high glucose concentration to low glucose concentration, while the second and third treatments comprised of a transition from low glucose concentration to high glucose concentration.

After each time-lapse, a .csv file of the FRET ratios calculated by Nikon Elements, the software packaged with the Nikon TI Eclipse, was used as the professional software control of this test. The images compiled by the microscope were then analyzed using the current imaging

algorithm and FRET ratios were collected. As the accuracy of the FRET ratios was not the primary focus of this experimental method, the trends between the FRET ratios from each respective algorithm were tested to determine if there was a significant difference in ability to detect change in FRET ratio between the two algorithms.

Characterization of Resolution and Contrast

The resolution and contrast of the microscope was determined empirically using a 1951 USAF resolution bar target. The resolution needs to be less than 5 μm. This would enable the microscope to effectively image specimens that are 5 μm in size. Specifically, the microscope should be able to image yeast cells, a single celled eukaryote commonly used to perform experiments in labs that are typically 5 to 10 μm in size [5].

Detecting Change in FRET Ratio

The FRET ratio in laconic sensors change by approximately by 10 percent when going when going from a high glucose solution to a low glucose solution and vice versa. Therefore, the microscope has to be able to detect at least a 10 percent change in the FRET ratio. To determine the change in FRET ratio the device could detect pancreatic islets cells infected with laconic were imaged at 535 nm and 470 nm in a 20 mM glucose solution. The images were then analyzed in ImageJ to determine the percent change in FRET ratio could be detected.

Results

Image Processing Algorithm Analysis

To evaluate the image processing algorithm implemented, time lapses of the CFP and YFP intensities of pancreatic islet cells exposed to the aforementioned treatments of varied

transitions between high (16.2 mM) and low glucose (2 mM) concentrations were plotted and recorded. Using the same image series, each treatment was analyzed with our own algorithm and the algorithm employed in Nikon Elements. The results of these treatments are depicted and summarized in Figure 2.

The treatments analyzed by both algorithms exhibited expected behavior based on the known effect of glucose on FRET ratios; that higher glucose concentrations yield greater CFP intensities and lower YFP intensities (high FRET ratios) while lower glucose concentrations yield lower CFP intensities and greater YFP intensities (low FRET ratios). After fitting each graph with a linear fit, eight slopes were gathered, two for each treatment, and a paired T-test was employed to determine if the eduFRET algorithm was statistically similar to the professional Nikon Elements algorithm. The null hypothesis projected a case in which there was no significant difference between the average FRET ratios between the software, while the alternate hypothesis suggested no significant difference between the two algorithms.

A P-value of 0.718 was calculated, suggesting there was no significant difference between the Nikon and the eduFRET software. While this conclusion is statistically relevant, it is important to consider the context of this P-value. With P-value's closer to 1, the results would suggest a greater resemblance between the team's algorithm and the professional software. Because of the lack of a more robust statistical result, a Bland-Altman statistical test will be run to provide a more accurate statistical conclusion about the efficacy of the algorithm. Unfortunately, due to the mismatch in sample numbers between the images analyzed by our software and Nikon Elements, this statistical test will not be able to be performed on this previously collected data, but future timelapse data with an equal number of samples for both algorithms will undergo this statistical test to provide better feedback on the algorithm's efficacy.

Characterization of Resolution and Contrast

The diffraction limited resolution was determined to be 0.4 μm using equation 1, where NA is the numerical aperture, 0.75, and λ is the wavelength of the excitation source in microns, 0.532.

$$Diffraction\ Limited\ Resolution(\mu m) = 0.61 * \frac{\lambda}{NA} \quad (1)$$

$$Empirical\ Resolution(\mu m) = \frac{1000}{2^{Group + (element-1)/6}} \quad (2)$$

Based on the USAF 1951 resolution chart, Figure 3A, the empirical resolution was determined to be 4.38 μm using equation 2; however, the width of the bar itself is 2.19 μm. Where 7 is the Group and 6 is the element.

A profile of group 7 element 6 created from the image of the resolution chart using ImageJ, Figure 3B. From the profile and equation 3, the contrast was determined to be 10.38%. Where I_{max} is the max pixel value, 192.9, of the sensor and I_{min} is the minimum pixel value, 156.6. See Figure 3B.

$$\%Contrast = \frac{(I_{max}-I_{min})}{(I_{max}+I_{min})} * 100 \quad (3)$$

Detecting Change in FRET Ratio Results

The FRET ratio, FR, measured from the islets was 0.6. The signal to background ratio in the 470 nm image was 1.5 while the signal to noise ratio in the 535 channel was 3.3. See Figure 4. The random noise at 500 ms exposure time in the both image channel was 7.5 counts out of 255 and the background, B.G, of in the images was 48 pixels out of 255. The pixel count in the 470 nm image,C_{470}, before accounting for background was 80 out of 255 and the pixel count for 535 nm image, C_{535}, was 160 out of 255. See Table 1. To determine the percent change in

FRET ratio the microscope could detect it was assumed the 535nm image pixel count would not change, and the 470nm image would account for the entire 10 percent change.

$$\frac{100}{FR}\left(\frac{C_{470}-B.G+Noise@500ms}{C_{535}}-\frac{C_{470}-B.G}{C_{535}}\right)=Percent\ Change\ in\ FRET\ ratio$$

Based on these assumptions it was calculated the microscope can detect a percent 11.2 percent change in FRET ratio.

Discussions and Conclusion

The eduFRET provides a cheaper alternative method for measuring FRET, providing a new opportunity for students and teachers to gain experience working with this microscopy technique. This proves particularly valuable in the fields of science and medicine where a majority of FRET research is conducted. FRET microscopy is limited by its cost, where microscopes range between $50,000 to $125,000 per scope, as estimated by Nikon. As a result, it is difficult for students at any level of their education to practice FRET. Prior studies have already shown the importance of hands-on experience within the STEM field. The eduFRET reduces the cost per scope to $10,000, making this technology more practical for implementation into the classroom. The increased accessibility to FRET microscopy could inspire more students to become involved in FRET, further advancing their understanding in biomedical and drug discovery research.

Characterization of Resolution and Contrast. The empirical resolution was based of microscope was based on the smallest set of bars the resolution target had available. Although the empirical resolution is 4.38 μm (see equation 2), the results indicated that the resolution is

closer to the width of the bars that are 2.19 μm. By imaging the resolution chart with even illumination and increasing the numerical aperture of the objective, the resolving power can be decreased.

The contrast is only 10.38 percent; however the contrast was measured on the smallest set group and element. Meaning this is the worst case contrast. When actual specimens are being imaged they will probably not be 2.2 μm near each other; therefore, the contrast during imaging will be better than 10.38%. The contrast could be improved by providing even illumination. During the imaging of the test chart, the chart was illuminated from above with an experimenter holding a flashlight, thus making the illumination uneven. Additionally, having an objective of a higher numerical aperture would also improve the contrast of the microscope. Future work will include determining the contrast and resolution of a research grade microscope.

Detecting Percent Change in FRET Ratio. The FRET ratio of a laconic sensor changes by 10 percent at most. The eduFRET microscope can only detect a 11.2 percent change; therefore, the current design of the microscope can not detect changes in FRET ratio. Improvements to the microscope can be made in order for the microscope to detect a percent change less than 10 percent. This can be done by switching to a 10 bit camera, using an objective with a higher numerical aperture or both. By switching to a 10 bit camera, assuming the same noise levels, the device would be able to detect a 2.1 percent change.

Future Work. To better characterize the optical system employed in the eduFRET microscope, the Modulation Transfer Function of the system will be gathered. With this information, an accurate estimation of the spatial resolution of the system will be calculated. Additionally, the timelapse series functionality and accuracy will be evaluated through the replication of several timelapse trials with our microscope and a Nikon TI Eclipse. These results

will be compared and assessed statistically to confirm the time lapse series efficacy. Lastly, the image processing algorithm will be tested through a Bland Altman test to verify the algorithm's qualitative accuracy.

Acknowledgments

We thank all the members of the Rogers Lab for their valuable contributions and suggestions, especially Zach Simmons for his guidance and suggestions. We also thank all the members of the Merrins Lab for their suggestions as well. We thank Michael Zupan for his help with the mechanical components of the scope. We thank Zach Alden for his suggestions to the design process of the eduFRET. We acknowledge the EI small grant fund.

Supplemental Material

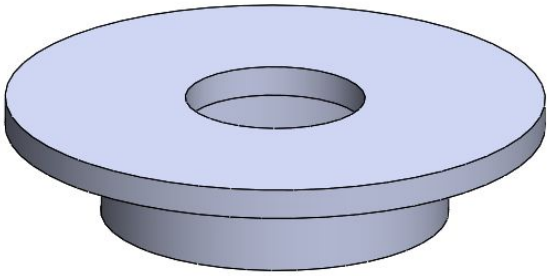

Figure S1. SolidWorks design of cell dish holder. A cell dish holder was printed in order to be able to rest a 1” petri dish that contains the cells. The bottom portion of the holder fits tight inside the focuser. The top hole is .75” will allow the cell dish to be moved around the top portion of the stand without falling through. The holder was printed at UW Madison’s MakerSpace using black PLA and PVA supports.

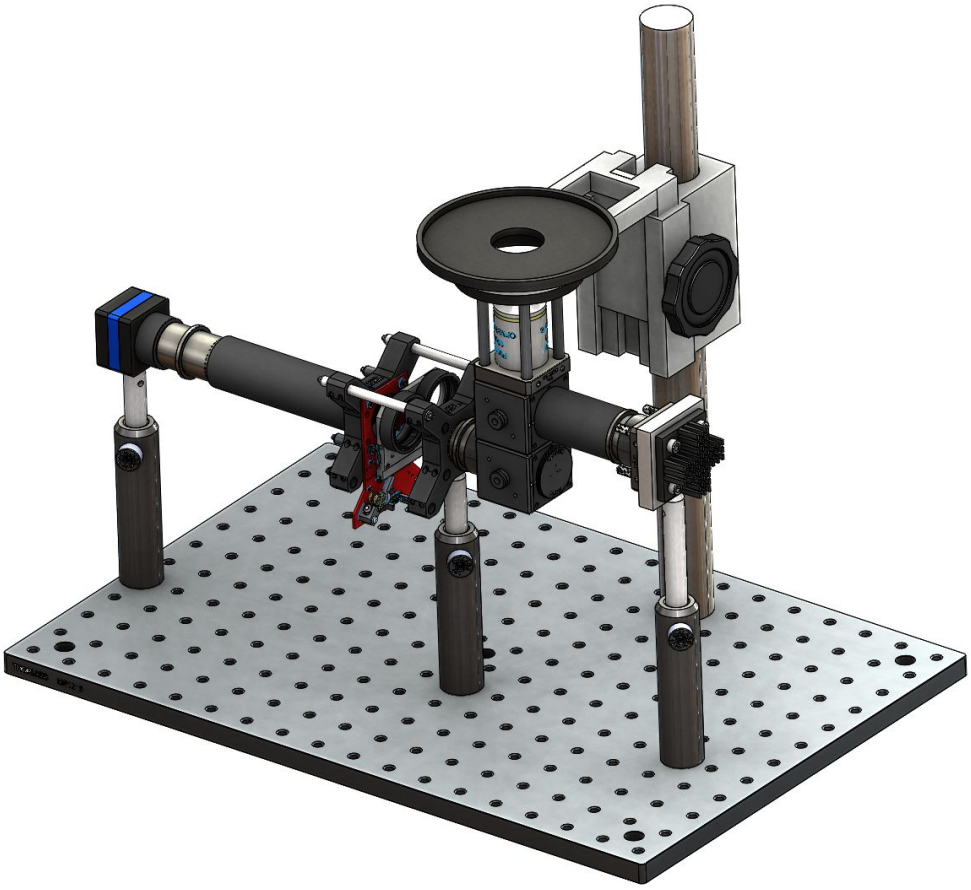

Figure S2. Computer aided design of eduFRET.The final assembly contains a triple bandpass dichroic mirror, fold mirror, filter cubes, 100 mm tube for light source. The additional parts assembled were purchased from various optic suppliers. The microscope contains an adjustable z-axis that will enable the user to attain a clear image of the cells. The top filter cube holds the dichroic mirror whereas the bottom filter cube holds the fold mirror. The microscope is secured on an optical board.

Figures

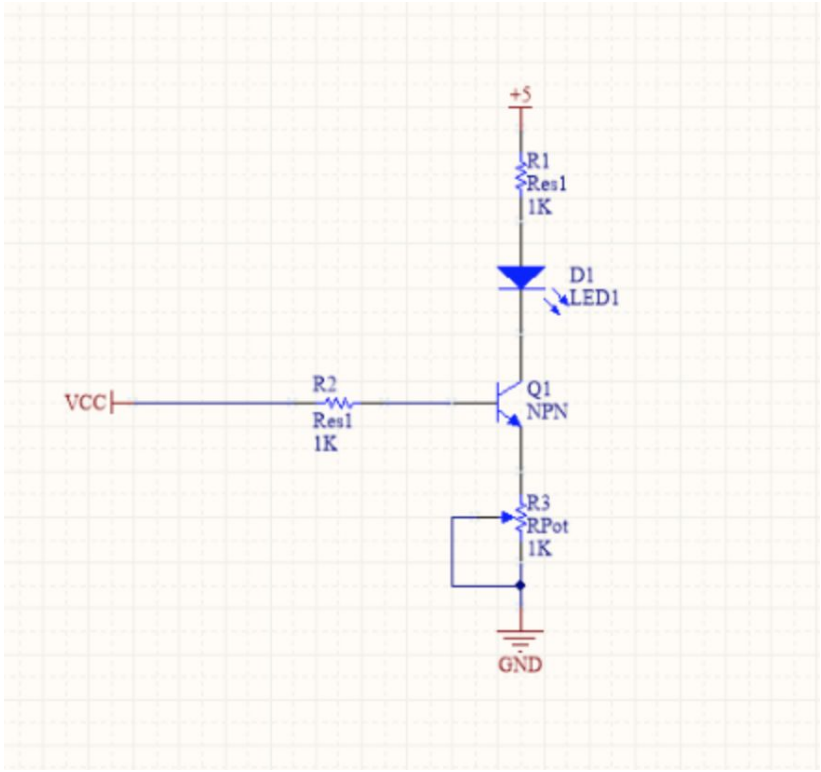

Figure 1.

The sample is excited by one 3W Vollong high powered 420 nm LED held in series with a 5Ω/3W resistor that can withstand the power output from the circuit. The high powered LED provides 200 lumens of light at its maximum output. The circuit is controlled by an Arduino Uno microcontroller which opens and closes an npn BJT transistor and also supplies 5V to the collector side of the BJT. A 10 kΩ potentiometer located on the emitter side of the BJT is used to control the current on the collector side of the device. The high-powered LED is connected to a 40.6 mm x 40.6 mm aluminum model heat sink purchased from digikey.com. All the resistors and transistor were purchased from Digikey.

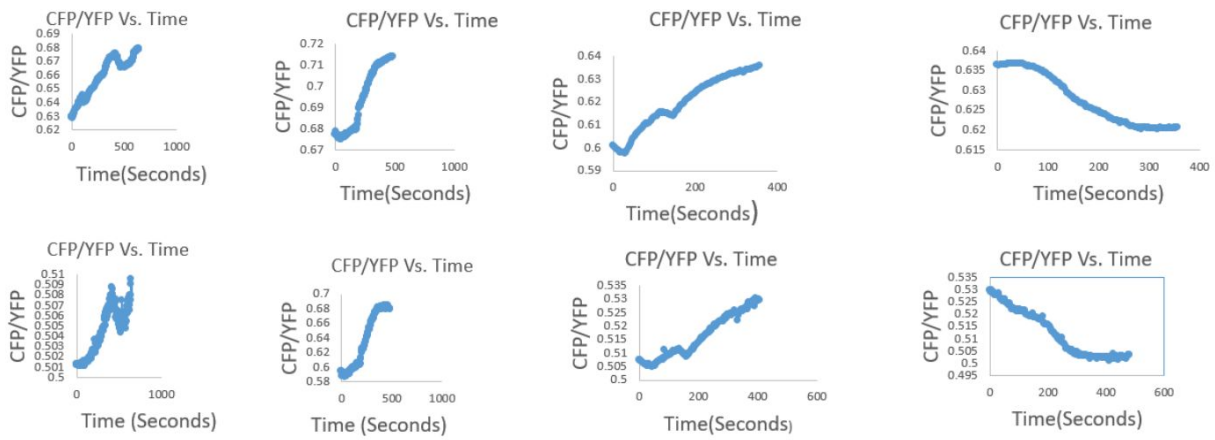

Figure 2

Top Row: FRET Ratio over time calculated by Nikon Elements. Bottom Row: FRET Ratio over time calculated with amateur software. From Left to Right: Low to High Glucose Concentration, Low to High Glucose Concentration, Low to High Glucose, High to Low Glucose. Note: CFP is equivalent to mTFP and YFP is equivalent to Venus in this specific case.

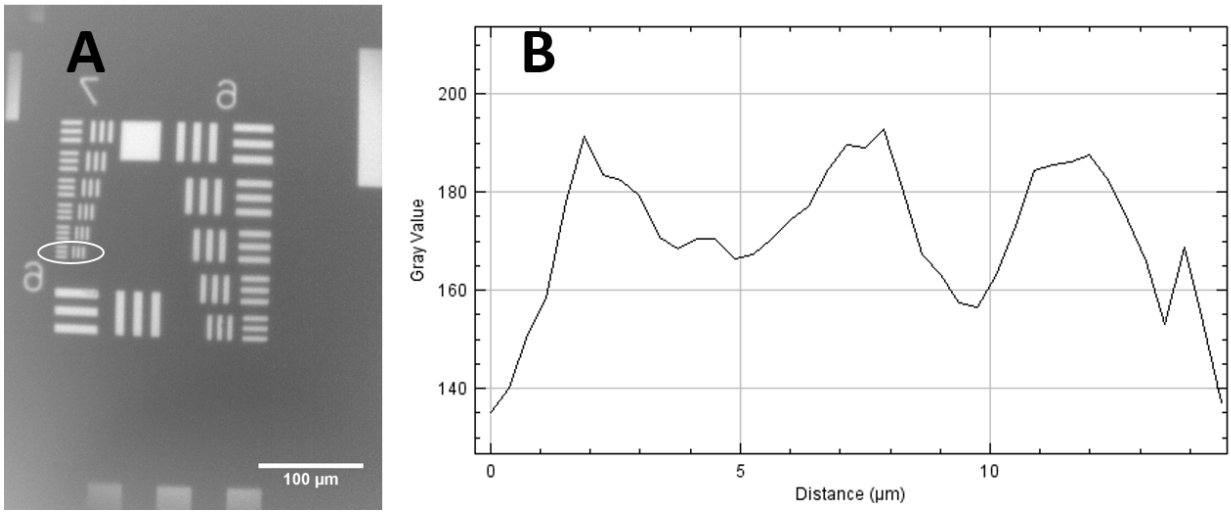

Figure 3.

Panel A is the 1951 USAF profile. The circle set of bars is Group 7 element 6. The bars themselves are 2.19 µm thick and the bars are spaced 4.38 µm apart. Panel B is the profile of vertical set of bars in group 7 element 6.

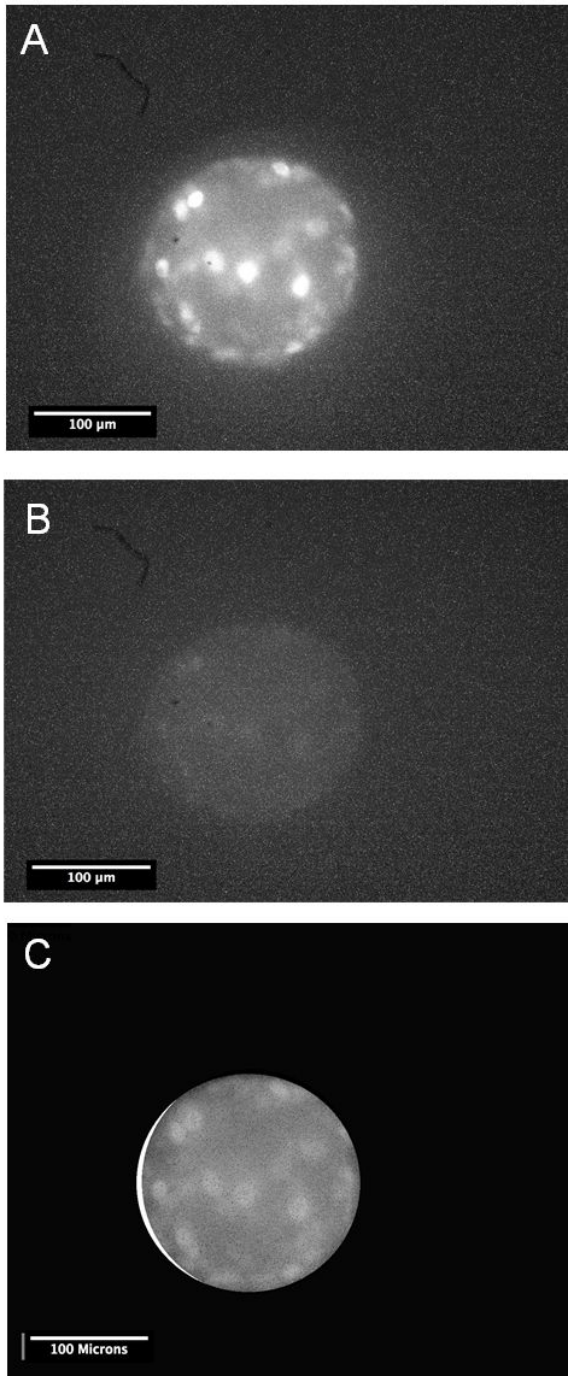

Figure 4.

Panel A is a pancreatic islet being imaged with a 535nm filter. Panel B is an islet being imaged with a 470nm filter. Panel C is the element wise division of the image in panel B by the image in Panel A.

Table 1.

Pixel Count of Islet at 470nm	80 out of 255
Pixel Count of Islet at 535nm	160 out of 255
Background	48 out 255
Noise	7.5 out of 255

References

[1] Tainaka K, Sakaguchi R, Hayashi H, Nakano S, Liew F, Morri T. Design Strategies of Fluorescent Biosensors Based on Biological Macromolecular Receptors. *Sensors* 2010; 10(2): 1355-76

[2] P. Mehrotra, "Biosensors and their applications – A review", *Journal of Oral Biology and Craniofacial Research*, vol. 6, no. 2, pp. 153-159, 2016.

[3] O. Shimomura, "The discovery of aequorin and green fluorescent protein", *Journal of Microscopy*, vol. 217, no. 1, pp. 3-15, 2005.

[4] B. Wu, K. Piatkevich, T. Lionnet, R. Singer and V. Verkhusha, "Modern fluorescent proteins and imaging technologies to study gene expression, nuclear localization, and dynamics", *Current Opinion in Cell Biology*, vol. 23, no. 3, pp. 310-317, 2011.

[5] A. Ibraheem and R. Campbell, "Designs and applications of fluorescent protein-based biosensors", *Current Opinion in Chemical Biology*, vol. 14, no. 1, pp. 30-36, 2010.

[6] B. Giepmans, "The Fluorescent Toolbox for Assessing Protein Location and Function", *Science*, vol. 312, no. 5771, pp. 217-224, 2006.

[7] R. Tsien, "Building and breeding molecules to spy on cells and tumors", *FEBS Letters*, vol. 579, no. 4, pp. 927-932, 2004.

[8] N. Shaner, P. Steinbach and R. Tsien, "A guide to choosing fluorescent proteins", *Nature Methods*, vol. 2, no. 12, pp. 905-909, 2005.

[9] J. Lippincott-Schwartz, "Development and Use of Fluorescent Protein Markers in Living Cells", *Science*, vol. 300, no. 5616, pp. 87-91, 2003.

[10] Zhang, R. Campbell, A. Ting and R. Tsien, "Creating new fluorescent probes for cell biology", *Nature Reviews Molecular Cell Biology*, vol. 3, no. 12, pp. 906-918, 2002.

[11] N. Aye-Han, Q. Ni and J. Zhang, "Fluorescent biosensors for real-time tracking of post-translational modification dynamics", *Current Opinion in Chemical Biology*, vol. 13, no. 4, pp. 392-397, 2009.

[12] A. Margineanu, J. Chan, D. Kelly, S. Warren, D. Flatters, S. Kumar, M. Katan, C. Dunsby and P. French, "Screening for protein-protein interactions using Förster resonance energy transfer (FRET) and fluorescence lifetime imaging microscopy (FLIM)", *Scientific Reports*, vol. 6, no. 1, 2016.

[13] Jares-Erijman E, Joven T. FRET imaging. *Nature Biotechnology* 2003;21:1387-95
[14] G. Allen, J. Kwak, S. Chu, J. Llopis, R. Tsien, J. Harper and J. Schroeder, "Cameleon calcium indicator reports cytoplasmic calcium dynamics in Arabidopsis guard cells", *The Plant Journal*, vol. 19, no. 6, pp. 735-747, 1999.

[15] A. Honda, S. Adams, C. Sawyer, V. Lev-Ram, R. Tsien and W. Dostmann, "Spatiotemporal dynamics of guanosine 3',5'-cyclic monophosphate revealed by a genetically encoded, fluorescent indicator", *Proceedings of the National Academy of Sciences*, vol. 98, no. 5, pp. 2437-2442, 2001.

[16] Y. Hwang, W. Chen and M. Yates, "Use of Fluorescence Resonance Energy Transfer for Rapid Detection of Enteroviral Infection In Vivo", *Applied and Environmental Microbiology*, vol. 72, no. 5, pp. 3710-3715, 2006.

[17] R. Kerr, V. Lev-Ram, G. Baird, P. Vincent, R. Tsien and W. Schafer, "Optical Imaging of Calcium Transients in Neurons and Pharyngeal Muscle of C. elegans", *Neuron*, vol. 26, no. 3, pp. 583-594, 2000.

[18] A. Miyawaki, J. Llopis, R. Heim, J. McCaffery, J. Adams, M. Ikura and R. Tsien, "Fluorescent indicators for Ca2+based on green fluorescent proteins and calmodulin", *Nature*, vol. 388, no. 6645, pp. 882-887, 1997.

[19] N. Mochizuki, S. Yamashita, K. Kurokawa, Y. Ohba, T. Nagai, A. Miyawaki and M. Matsuda, "Spatio-temporal images of growth-factor-induced activation of Ras and Rap1", *Nature*, vol. 411, no. 6841, pp. 1065-1068, 2001.

[20] A. Tanimura, A. Nezu, T. Morita, R. Turner and Y. Tojyo, "Fluorescent Biosensor for Quantitative Real-time Measurements of Inositol 1,4,5-Trisphosphate in Single Living Cells", *Journal of Biological Chemistry*, vol. 279, no. 37, pp. 38095-38098, 2004.

[21] Ha, J. Song, Y. Lee, S. Kim, J. Sohn, C. Shin and S. Lee, "Design and Application of Highly Responsive Fluorescence Resonance Energy Transfer Biosensors for Detection of Sugar in Living Saccharomyces cerevisiae Cells", *Applied and Environmental Microbiology*, vol. 73, no. 22, pp. 7408-7414, 2007.

[22] Lippincott-Schwartz, E. Snapp and A. Kenworthy, "Studying protein dynamics in living cells", *Nature Reviews Molecular Cell Biology*, vol. 2, no. 6, pp. 444-456, 2001.

[23] A. San Martín, S. Ceballo, I. Ruminot, R. Lerchundi, W. Frommer and L. Barros, "A Genetically Encoded FRET Lactate Sensor and Its Use To Detect the Warburg Effect in Single Cancer Cells", *PLoS ONE*, vol. 8, no. 2, p. e57712, 2013.

[24] M. Merrins, A. Van Dyke, A. Mapp, M. Rizzo and L. Satin, "Direct Measurements of Oscillatory Glycolysis in Pancreatic Islet β-Cells Using Novel Fluorescence Resonance Energy Transfer (FRET) Biosensors for Pyruvate Kinase M2 Activity", *Journal of Biological Chemistry*, vol. 288, no. 46, pp. 33312-33322, 2013.

[25] R. Heim and R. Tsien, "Engineering green fluorescent protein for improved brightness, longer wavelengths and fluorescence resonance energy transfer", *Current Biology*, vol. 6, no. 2, pp. 178-182, 1996.

[26] R. Day, C. Booker and A. Periasamy, "Characterization of an improved donor fluorescent protein for Förster resonance energy transfer microscopy", *Journal of Biomedical Optics*, vol. 13, no. 3, p. 031203, 2008.

References

1. Tainaka K, Sakaguchi R, Hayashi H, Nakano S, Liew F, Morri T. Design Strategies of Fluorescent Biosensors Based on Biological Macromolecular Receptors. sensors 2010; 10(2): 1355-76
2. Jares-Erijman E, Joven T. FRET imaging. Nature Biotechnology 2003;21:1387-95
3. San Martin A, Ceballo S, Ruminot I, Lerchundi R, Frommer W, Barros L. A Genetically Encoded FRET Lactate Sensor and Its Use To Detect the Warburg Effect in Single Cancer Cells. PLoS one. 2013; https://doi.org/10.1371/journal.pone.0057712
4. Ohta J. Smart CMOS Image Sensors and Applications. Taylor & Francis; 2007. P. 15-17
5. Kaiser, Gary E. Biol 230 Lab Manual, Lab 1. Community College of Baltimore County. 29 May 2000